Magnetic Characterization of CrO_2 Tape Coatings

by Randy Lee

Feburary, 1994

Graham Magnetics

INTRODUCTION

Chromium dioxide, because of its unique magnetic properties, is used extensively for magnetic tape applications. Tapes made with CrO_2 can record more information and are capable of reproducing high frequency signals better than conventional tapes using γ-Fe_2O_3. Crystals of CrO_2 are synthesized under high pressure and temperature to form dendrite-free particles of about 10:1 aspect ratio[1]. In recording media, CrO_2 particles can be packed closer together than particles of γ-Fe_2O_3 because of their morphology. However, it has been observed for both systems that an increase in the magnetic oxide content causes a corresponding decrease in measured coating coercivity. This is believed to be due to an increase in negative *interparticle interactions* accompanying the increase in volume packing fraction.

For this study, effects associated with variations in the CrO_2 content of MTC-type formulated coatings are investigated with respect to their bulk magnetic properties. Results indicate that the concentration of CrO_2 plays an insignificant role in the time required to effectively mill a given slurry to the first letdown. This is in contrast to γ-Fe_2O_3 Epoch-based formulations in which the γ-Fe_2O_3 concentration has been shown to have a significant effect on the milling time[2]. The results do however, reflect a large variation in the coated magnetic properties with respect to the CrO_2 concentration.

The discussion portion of this report is presented in two sections:
Section I - Mill Time Evaluation
Section II - Post Coat Analysis
The primary goals of Section I are to compare differences in the magnetic properties over milling time for several CrO_2 loading levels and to illustrate the optimum (or model) time values for each of the magnetic properties monitored throughout the process. The primary goals of Section II are to define bulk coating magnetic properties in terms of CrO_2 concentration and to offer a possible explanation for the anomalous decrease in coating coercivity with increasing CrO_2 concentration based on the interparticle interaction field.

EXPERIMENTAL

Five CrO_2 concentration loading values between 58% and 90% were pre-selected as illustrated in Figure 1.

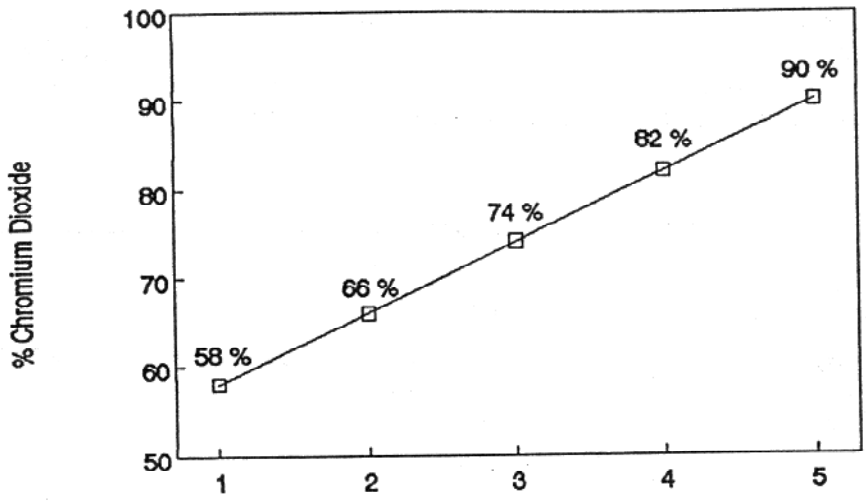

Figure 1. Target CrO_2 loading concentrations. The standard MTC loading is 80.5%.

Actual loading concentrations were 58.0%, 65.7%, 74.0%, 82.0%, and 88.3% respectively. Each load variation, formulated and processed separately, consisted of CrO_2 particles, polyester/urethane resin-binder, lubricants and wetting agents (in proportion to the CrO_2 content). Each batch was processed through the #14 sand mill and targeted to produce several thousand grams of slurry for coating several hundred feet of film. The number of passes through the sand mill for each Phase I formulation varied between 8 and 10 passes. Elapsed time between the second letdown and coating varied from mill to mill due to scheduling differences. Also, the amount of solvent added and the point of addition varied for each mill depending on the working consistency of the slurry.

Magnetic characterization was performed throughout the milling process and after coating using the LDJ model 7500A B-H meter. In-process measurements were taken before (or after) each pass. Post-coated magnetic results are an average of a minimum of three measurements performed on as-coated film. Bulk coating density and particle volumetric packing fraction were determined geometrically and are given as an average of a minimum of three measurements performed on as-coated film. The rolls were slit and submitted for signals testing on the 3480 MTC tester. Samples were also submitted for surface roughness measurements.

Acknowledgements: John Meeks (Process Engineer) performed and oversaw the major portion of each milling process. Larry Bundrick and Jimmy Logan (Process Technicians) were responsible for performing the third letdown phase, pre-coat slurry filtration and the complete coating process. All magnetic and bulk test data and measurements presented in the report were taken by the same operator throughout.

RESULTS AND DISCUSSION

SECTION 1 - Mill Time Evaluation

Magnetic properties were tabulated throughout the milling process. Plots of each magnetic property against milling time (number of passes or pass number) were generated and compared. No apparent gradient in magnetic properties over milling time was observed for CrO_2 as seen with γ-Fe_2O_3 in an earlier study[2]. For the most part, data points between batches over mill time were diffused or indistinct as illustrated in Figure 2 for the coercivity and squareness.

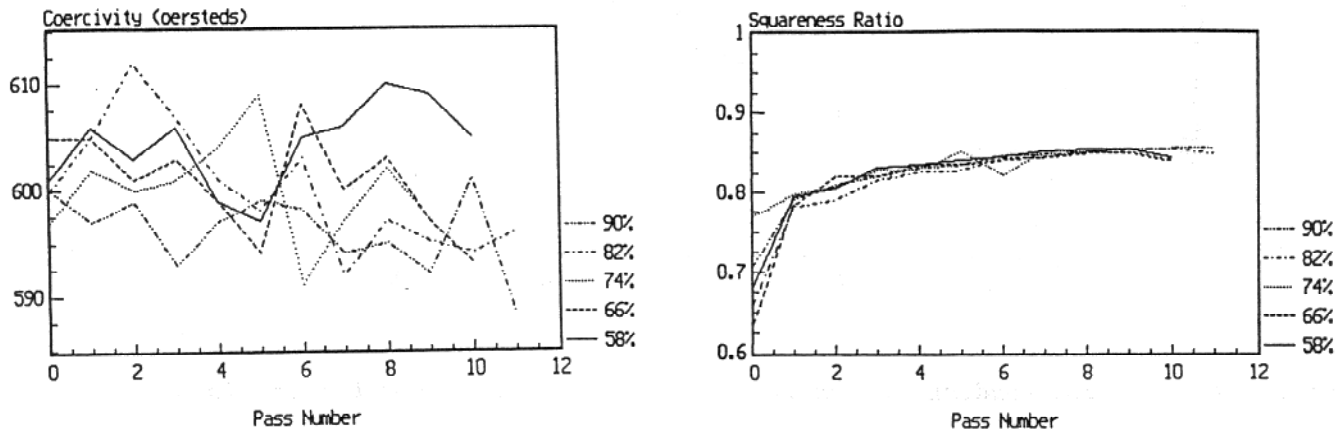

(a) Hc vs. pass number

(b) Sq vs. pass number

Figure 2. Changes in Hc and Sq over milling time for the five loading variations.

It is therefore concluded that *the concentration of CrO_2 in the range 58-90% has no significant effect on the time required to mill a given slurry to the first letdown.* Rather than present graphs for all the magnetic properties here, it is appropriate to show the raw data averages in Figure 3 where the properties at each mill point are averaged over all five loading concentrations.

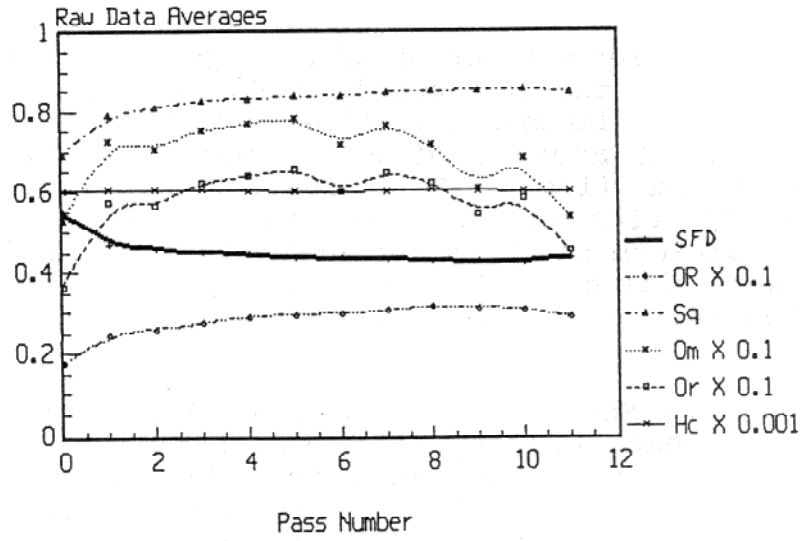

Figure 3. Unitized averages of magnetic properties for 58% - 90% CrO_2 concentration.

From Figure 3, the squareness Sq, orientation OR, and switching field distribution SFD seem to level off at some maximum or minimum value. However, a closer look reveals that the extremes actually occur during a small parabolic change between about pass 7 and pass 11. A similar case was observed for the coercivity with γ-Fe_2O_3 dispersions investigated previously. The flux (ϕ_r and ϕ_m) also appears to change parabolically but over the entire milling time, and the coercivity H_c continuously decreases over the entire time range. If quadratic functions are used to emulate each property, then model curves can be constructed to illustrate their behavior over the specified time range (pass number). Also, setting the derivative of each function to zero gives the peak time or optimum number of passes for each property. For example, a magnetic property N undergoing n passes is written

$$N = c + bn + an^2$$

where

$$n_{peak} = \frac{-b}{2a}$$

Model curves for H_c, ϕ_r and ϕ_m from zero through pass 11, and OR, Sq and SFD from pass 7 through pass 11 are depicted in Figure 4. Table 1 gives computer curve fits and the peak pass number for each property over milling time (number of passes through the sand mill).

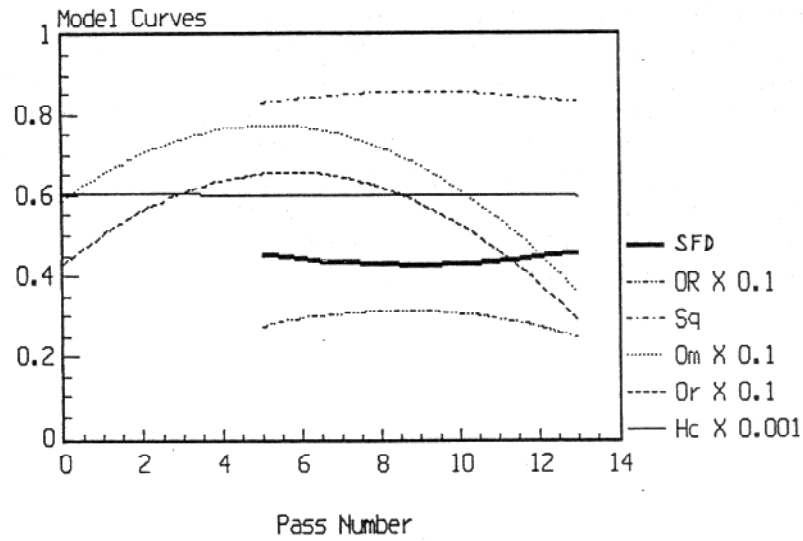

Figure 4. Optimized data for CrO_2 magnetic properties over milling time.

Table 1. Functional curves for CrO_2 magnetic properties and peak pass number.

Model Functions	dP/dn = 0
$H_c = 602 - 0.090n - 0.021n^2$	$n_{peak} = -2.2$
$\phi_r = 4.29 + 0.788n - 0.069n^2$	$n_{peak} = 5.7$
$\phi_m = 5.88 + 0.706n - 0.068n^2$	$n_{peak} = 5.2$
$OR = 0.926 + 0.526n - 0.031n^2$	$n_{peak} = 8.4$
$Sq = 0.724 + 0.028n - 0.002n^2$	$n_{peak} = 9.0$
$SFD = 0.577 - 0.034n + 0.002n^2$	$n_{peak} = 8.9$

The optimum milling time for H_c is negative because this property continually decreases throughout the milling process. H_c can be regarded as a relative indication of the average particle (or agglomerate) size in the collection of particles that make up the coating. As the milling process gradually reduces the average particle length, H_c decreases accordingly. The SFD is a measure of the average *variation* in particle length. It's theoretical maximum value of 0.5 corresponds to the situation where the particle sizes range from very small ellipsoids to long needles and elongated agglomerates. When the SFD is zero, all the particles are identical in shape and size. Even though a SFD of zero is completely unrealistic, the lowest possible SFD value attainable is the desired goal. However, over-milling produces a situation where the individual particles begin to break up thus widening the SFD range. It is this point that marks the best milling time for both SFD and Sq. A wide variation in particle sizes produces a low Sq because the retained alignment is more difficult than remanent alignment of identical particles. Hence, the optimum milling time (or number of passes) is represented by the point where milling has reduced the agglomerates without significantly degrading the individual particles.

SECTION II - Post-Coat Analysis

Using unslit coated samples, typical magnetic properties were determined by taking measurements on several samples at each oxide level. The averages are given in Table 2 and plotted in Figure 5a. After slitting, signal data was generated on the MTC test machine relative to the standard GMI-574. Only the input write current (% of standard), output voltage amplitude (% of standard), and signal-to-noise ratio were considered. Results are shown in Table 2 and plotted in Figure 5b.

Table 2. Average post-coat magnetic properties for 58% - 90% CrO_2 content.

	58.0%	65.7%	74.0%	82.0%	88.3%	Production
Coercivity (Oersteds)	607	595	592	591	581	628
Remanent Flux (Maxwells)	1.55	2.11	2.01	2.25	2.27	2.28
Maximum Flux (Maxwells)	1.83	2.50	2.35	2.64	2.66	2.62
Squareness	0.847	0.842	0.855	0.852	0.853	0.871
Orientation Ratio	3.08	2.97	3.22	3.04	3.03	3.51
Switching Field Distribution	0.435	0.432	0.420	0.412	0.406	0.430
Write Current (% of SRM)	108.7	101.7	100.1	96.6	100.6	101
Output Voltage (% of SRM)	46.8	44.0	79.5	86.4	98.8	88
Signal-To-Noise Ratio (dB)	29.2	30.4	32.5	33.8	36.2	34

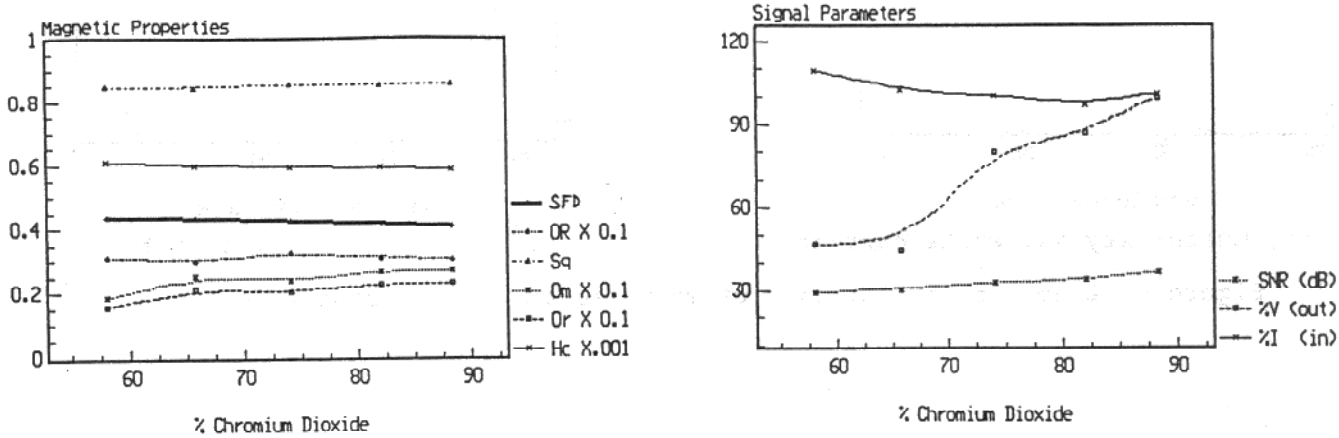

(a) Magnetic Properties (b) Signal Data

Figure 5. Average post-coat magnetic properties for 58% - 90% CrO_2 content.

As tabulated in Table 2 and illustrated in Figure 5b, the relative write current decreases slightly as the level of CrO_2 increases from 58% to 88.3%, and the relative output increases significantly from 58 to 88%. Also, the signal-to-noise ratio (SNR) increases steadily over the test range. As expected, all three changes represent an improvement in performance characteristics as the oxide level is increased. In terms of signal response, the ideal or optimum oxide loading can be indicated in a manner similar to that employed for the optimum milling time in Section I. Obviously, the highest output and SNR that can be obtained are desired goals. For this task however, the lowest possible input level is considered to be the critical parameter. Fitting a parabolic curve to the write current data in Figure 5b (upper curve), gives the equation $\%I = 0.0238p^2 - 3.771p + 248.2$ where p is the $\%CrO_2$. When the derivative is set to zero, p = 79.2% which coincides well with the production value of 80.5%.

When the efficiency constants are known for a given head, the absolute write current (in Amps) is considered to be proportional to the H-field within the head-to-tape gap. Also, for constant frequency and tape speed, Faraday's law defines the absolute output (in Volts) to be proportional to the flux.[3] In a similar manner, it is interesting to note the approximate linear relationships that are apparent with the coercivity values in this study to the write current, and the squareness values to the output data. Given the degree of scatter in the coercivity and output results, 0.999 curve fits are not expected however, Figure 6a and 6b will serve to illustrate this apparent linearity.

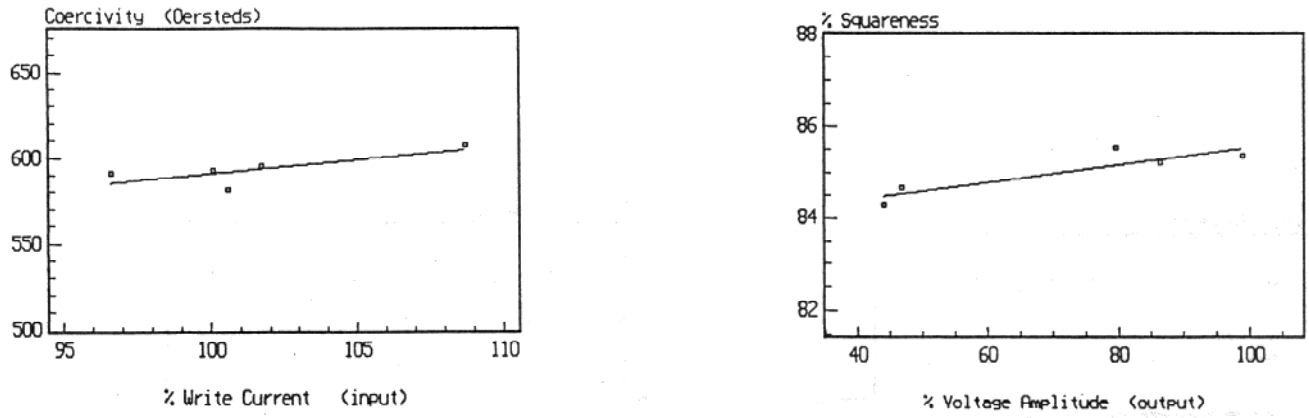

(a) Coercivity vs. write current (b) Squareness vs. output

Figure 6. Linear representative of magnetic and signal properties.

Referring now back to Figure 5a, two relevant magnetic features can be noted: (1) both H_c and SFD decrease continuously as the CrO_2 content increases from 58 to 90%. This trend can be accounted for by the interparticle interaction field. (2) ϕ_r, ϕ_m, Sq and OR appear to increase with $\%CrO_2$ but not with the same degree of continuity as H_c and SFD. Continuity breaks appear to occur between 65.7% and 74%. These irregularities may be attributed to nonuniform bulk characteristics of the coating which can be further examined after determination of the bulk coating density and magnetic particle volume fraction.

Original derivations of the following formulas are given in Section I of the Appendix. The magnetic particle volume fraction p_v can be estimated when the bulk coating density ρ_c and magnetic particle density ρ_p are known,

$$p_v = p_w \frac{\rho_c}{\rho_p}$$

where p_w is the magnetic particle weight fraction taken directly from the Formulation Worksheet. Bulk coating densities were measured geometrically for each load variation as well as on production samples. The bulk particle density for CrO_2 is taken as 4.8 g/cm^3 [4].

The *matrix* pertains to all components in the coating except the magnetic particles and the porosity. The non-porous (or real) matrix density ρ_m is given as

$$\rho_m = \left[\frac{r_w \rho_r^{-1} + s_w \rho_s^{-1} + l_w \rho_l^{-1} + \ldots}{m_w} \right]^{-1}$$

where r_w, s_w, l_w, ... are the component weight fractions for resin, surfactants, lubricants, ... taken directly from the Formulation Worksheet while ρ_r, ρ_s, ρ_l, ... are their respective densities as taken from vendor reports and MSDS sheets. Also, m_w is the total matrix weight fraction taken directly from the Formulation Worksheet ($m_w = 1 - p_w$).

An expression for the apparent porosity or air volume α is

$$\alpha = 1 - \rho_c \left[\frac{p_w}{\rho_p} + \frac{m_w}{\rho_m} \right]$$

Finally, the pigment (or particle) volume concentration PVC is given by

$$PVC = \left[1 + \frac{m_w}{p_w} \cdot \frac{\rho_p}{\rho_m} \right]^{-1}$$

If coating thickness and bulk density are precisely measured, p_v, ρ_m, α and PVC can be approximated. Table 3 gives measured and calculated post-coated bulk properties for the five loading variations.

Table 3. Average post-coated physical properties for 58% - 90% CrO_2 content.

	58.0%	65.7%	74.0%	82.0%	88.3%	Production
Measured Thickness (μ inches)	158	158	138	118	118	118
Bulk Coating Density (g/cm^3)	1.860	2.280	2.110	2.542	2.453	2.649
Real Matrix Density (g/cm^3)	1.155	1.138	1.112	1.067	0.996	1.078
Apparent Porosity (%)	9.89	0.072	18.1	13.7	26.0	7.98
Particle Volume Fraction (%)	22.5	31.2	32.5	43.4	45.1	44.3
Pigment Volume Concentration (%)	25.0	31.2	39.7	50.3	61.0	48.1

As indicated earlier, discrepancies in the flux and squareness between 65.7% and 74.0% were linked to nonuniform bulk coating variations. This is clearly reflected in the values for the measured bulk coating density and somewhat in the particle volume fractions and porosity values. The porosity (voids and airspace) seems rather high for some cases but his property cannot be measured easily for tape coatings. It is highly dependent on the kind of intrusion material used in it's determination. The table values are only considered as rough estimates that are very sensitive to the specific numbers used for the matrix density.

The matrix density, being based primarily on MSDS reported values, is subject to uncertainty since the actual density of any isolated component is dependent on the conditions of temperature, pressure and chemical activity it sees during processing. For instance, the wetting agent Centrolex-P, comes in the form of highly porous granules (0.47 g/cm^3 bulk density) whose true or *milled* density is unknown but is definitely higher than 0.47. Also, the crosslinker CB-701, and catalyst $Fe(AA)_3$, are reactive components whose reported densities become irrelevant during the coating process.

Professional and journal reported estimates of volumetric packing fraction for CrO_2 tapes ranges from 32-47% indicating that the values in Table 3 for p_v are quite significant. Analogous to the bulk coating density, the packing fraction is indicative of the bulk magnetization of a coating as will be shown.

According to principles in pigment/binder geometry [5], the pigment volume concentration PVC, should equal the packing fraction at all points below the critical pigment volume concentration CPVC, (the point where matrix just fills all the porosity). Below the CPVC, the coating is over filled with matrix, the particles are separated and no voids or air space are present. Above the CPVC, the particles are in intimate contact, the coating is matrix (or resin) starved and pore volume makes up a measurable amount of the total coating volume. Any coating with a porosity fraction has the condition CPVC = p_v. According to Table 3, the oxide loading at 65.7% would be close to the point corresponding to CPVC but then the 58.0% loading should have zero porosity since there is an abundance of matrix. Clearly, this is not the case. It is possible the matrix may become inherently porous due to some operation in the milling process. Also, the presence of pores and voids in the magnetic particles themselves has not been considered. Whatever reasons this data does not exactly conform to pigment/binder theory will not be investigated here. Suffice it to say that in all five cases, CPVC = p_v.

From Table 3, a plot of p_v against p_w for the range 58.0% to 88.3% is shown in Figure 7a along with a linear approximation. The zigzag appearance is due to limitations in the thickness measure device. The actual behavior of p_v over the entire range 0-100% is expected to follow a curve similar to that given in Figure 7b which includes the zero point where the packing fraction is known to be zero when there are no particles present.

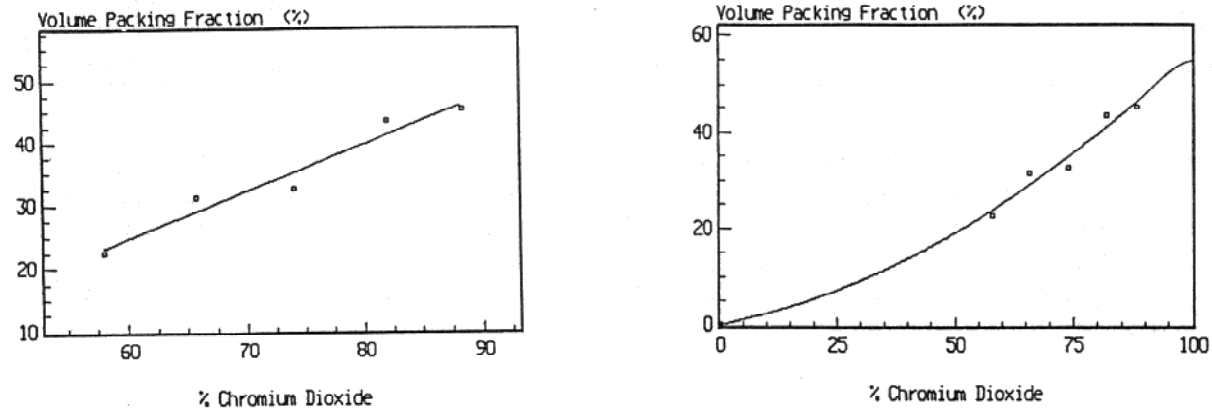

(a) Linear approximation (b) Expected function

Figure 7. Variation of volume packing fraction with % CrO_2.

This might resemble one-half of a second order exponential or Gaussian type function. In any case, p_v must taper off as the particles begin to make contact with each other. A similar situation is found with the bulk coating density ρ_c where the zero point consists only of matrix very close to the vendor reported resin density of 1.2 g/cm^3. Of all the reported component densities, the one for solid thermoplastic resin pellets is the most reliable since this form is probably very close to its form in the finished coating.

The bulk coating *magnetization* is expected to behave in the same manner as p_v and ρ_c. Before discussing bulk coating magnetization, a review of Section II in the Appendix is suggested which clarifies the magnetic units used in this report.

For the present study, it has been found that the *bulk* coating magnetization is equal to the measured coating flux divided by the product of the coating thickness t and the sample width (a constant of 5 cm). So the remanent and maximum coating magnetization are given respectively by

$$M_r = \frac{\Phi_r}{5t} \quad \text{and} \quad M_m = \frac{\Phi_m}{5t}.$$

The vendor (VSM) reported value for specific saturation magnetization or saturation moment for CrO_2 particle is (73 emu/g)[1]. Table 4 gives the remanent magnetization M_r and maximum magnetization M_m based on the measured coating flux and thickness for the five CrO_2 variations and the production average.

Table 4. Remanent and maximum magnetization as a function of coating flux.

	58.0%	65.7%	74.0%	82.0%	88.3%	Prod.
M_r (Gauss)	772	1051	1147	1501	1515	1522
M_m (Gauss)	912	1247	1341	1762	1775	1748

The squareness is defined as the ratio of M_r to M_m, $Sq = M_r/M_m$, and represents the fraction (or percentage) of bulk coating magnetic moment that remains aligned in the direction of the applied field H, after H is removed. The directions of H and M_m are the same but are at an angle e_r to M_r. So the Sq can be considered as a measure of the average angle between M_r and M_m

$$\theta_r = \arccos(Sq)$$

Remanent angles for each loading can be calculated but do not reflect the variation in coating remanence as well as the squareness values.

From Table 4, a plot of M_r against p_w for the test range 58.0% to 88.3% is given in Figure 8a. Analogous to p_v and p_c, the actual behavior of M_r (or M_m) is expected to follow a curve similar to that shown in Figure 8b over the range 0-100%. Indeed, M_r is expected to be highly dependent on the coating density and most importantly, on the magnetic particle volume fraction. For the test range however, M_r could be approximated by a straight line.

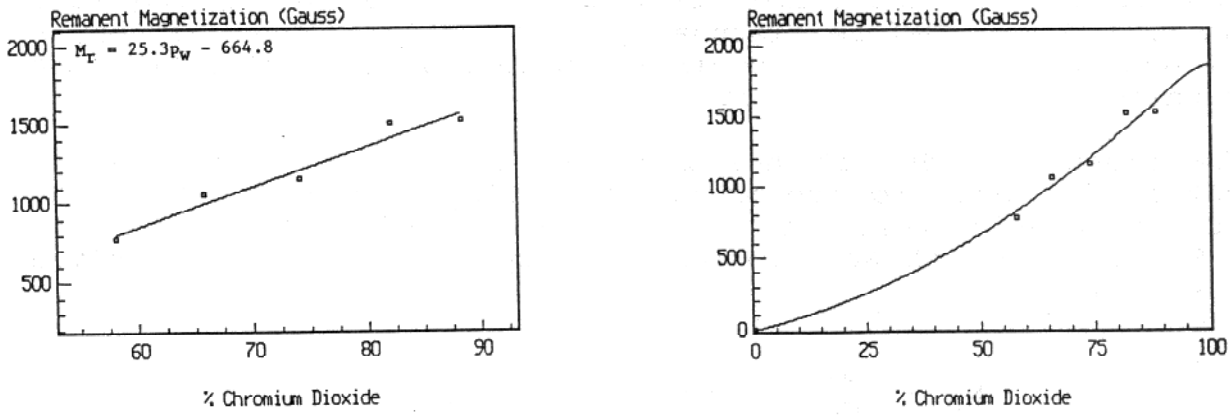

(a) Linear approximation (b) Expected function

Figure 8. Variation of bulk coating magnetization with % CrO_2.

The switching field distribution SFD is a measure of the average fractional deviation in individual particle coercivity with respect to the measured mean H_c or simply the percentage deviation. Thus the SFD is the reduced switching field,

$$SFD = \frac{H_s}{H_c}$$

where H_s represents the average switching field. The individual particle coercivity can range anywhere from $(H_c + H_s)$ to $(H_c - H_s)$ so $2 \cdot SFD$ might be regarded as the switching *range* distribution. Values for H_s are given in Table 5. From Table 2, H_c is plotted against p_w (CrO_2 content) and given in Figure 9a. As seen in Figure 9b, linearization is greatly improved when H_s is given as a function of p_w.

Table 5. Measured switching fields for 58 - 90% CrO_2.

	58.0%	65.7%	74.0%	87.0%	88.3%	Production
H_s (Oersteds)	264	257	249	243	236	270

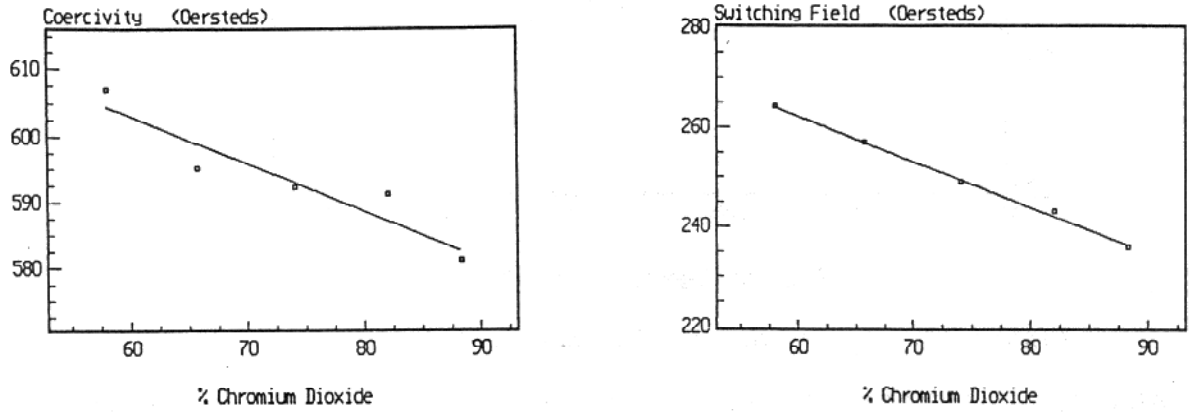

(a) H_c vs. CrO_2 (b) H_s vs. CrO_2

Figure 9. Average coating coercivity land switching field vs. CrO_2 content 58-90%.

The downward trends depicted in graphs 9a and 9b can be accounted for by the remanent interparticle interaction field H_i which represents the classical magnetostatic interaction between particles after saturation. Like the SFD and H_s, H_i is only a measure of the *average* interaction field between particles and has been estimated by other workers via delta-M measurements [6]. Positive interactions have been observed for BaFe due to "stacking" of the platelet-shaped particles. However, negative interactions are characteristic of acicular particles because the overall interaction effect is more of repulsion than attraction.

For this study, H_i can be estimated by recalling that both M and H_s are treated as linear functions of p_w in the range 58-90%. It is customary to assume that H_i is directly proportional to the magnetization.[7] Since *remanent* particle interaction is the field of interest then

$$H_i = kM_r$$

The constant k can be estimated by considering H_i to be proportional to the negative change in H_s over M_r that is, as M_r increases with increasing p_w, H_i increases at the same rate that H_s decreases, so

$$k = \frac{dH_s}{dM_r}$$

The numerical value of k can be taken as the slope of the graph in Figure 10 showing H_s as a function of M_r.

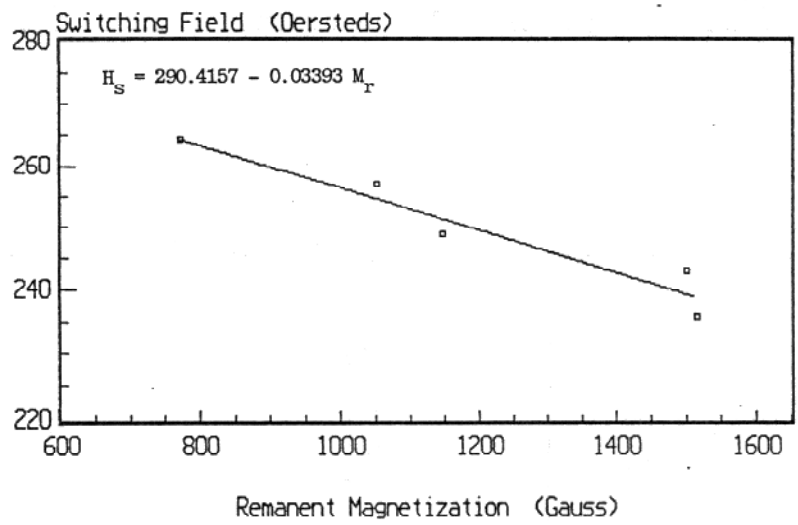

Figure 10. H_s vs. M_r for the range 58%-90% CrO_2.

For this study, the interparticle interaction field is effectively represented by

$$H_i = -0.03393\, M_r(p_w)$$

where the negative sign is indicative of the repulsive interparticle interaction field between the acicular particles. Functional values for $M_r(p_w)$ are given in Figure 8a and the calculated H_i values are shown in Table 6. The change in H_c and H_s are very similar so that either dH_c/dM_r or dH_s/dM_r could be used to approximate the value for k. For this particular study however, H_s gives á better fit with the data and is therefore considered to be more adequate for representing the change in the H-field with the magnetization. Also, M_r (p_w) is used in the calculation of H_i because of its smoothing effect over the thickness dependent M_r numbers.

Table 6. Estimated interparticle interaction fields for 58%-90% CrO_2.

	58.0%	65.7%	74.0%	82.0%	88.3%	Prod.
H_i (Oersteds)	27.2	33.8	41.0	47.8	53.2	46.5

The H_i value given in Table 6 for production is in excellent agreement with the remanent interaction fields determined by other workers for CrO_2 tapes.[6] Values for 58%-90% vary with packing fraction as expected and are illustrated in Figure 11 where table values are plotted with the theoretical point $H_i = 0$ for $p_v = 0$.

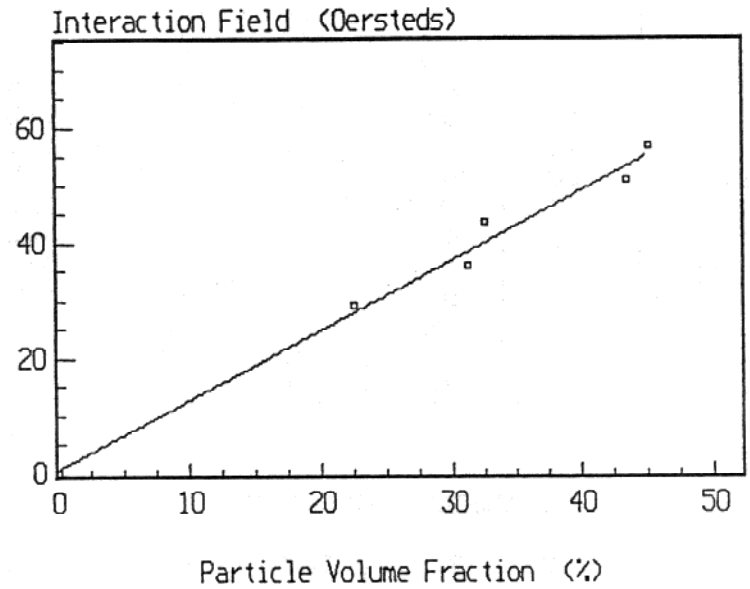

Figure 11. Interparticle interaction field vs. volumetric packing fraction extrapolated to zero.

The significance of Table 6 is realized by adding each H_i value to its corresponding coercivity from Table 2 which equals almost the same value across the 58%-90% range. The average is 634 Oersteds which represents the mean single particle coercivity corresponding to zero interparticle interaction. Then for needle shaped particles,

$$H_i = h_c - H_c$$

where h_c is the single particle coercivity of an *average* particle. Thus, spherically shaped particles would have $H_c = h_c = H_i = 0$. For platelet particles, the coating coercivity is much higher than the individual particle coercivity and the *positive* interaction field is written as $H_i = H_c - h_c$. In conclusion, H_c can be considered as the average coercivity of an individual particle *after* the H_i field is accounted for, where H_i is a measure of the demagnetization effect between particles. A complete tabulation of test data and calculated results for this report are given in Table 7.

Table 7. Magnetic and physical properties for 58-90% CrO_2.

MAGNETIC & ELECTRICAL PROPERTIES

	58.0%	65.7%	74.0%	82.0%	88.3%	Production
Coercivity (Oersteds)	607	595	592	591	581	628
Remanent Flux (Maxwells)	1.55	2.11	2.01	2.25	2.27	2.28
Maximum Flux (Maxwells)	1.83	2.50	2.35	2.64	2.66	2.62
Squareness	0.847	0.842	0.855	0.852	0.853	0.871
Orientation Ratio	3.08	2.97	3.22	3.04	3.03	3.51
Switching Field Distribution	0.435	0.432	0.420	0.412	0.406	0.430
Write Current (% of SRM)	108.7	101.7	100.1	96.6	100.6	101
Output Voltage (% of SRM)	46.8	44.0	79.5	86.4	98.8	88
Signal–To–Noise Ratio (dB)	29.2	30.4	32.5	33.8	36.2	34
Remanent Magnetization (Gauss)	772	1051	1147	1501	1515	1522
Maximum Magnetization (Gauss)	912	1247	1341	1762	1775	1748
Switching Field (Oersteds)	264	257	249	243	236	270
Interaction Field (Oersteds)	27.2	33.8	41.0	47.8	53.2	46.5

BULK PHYSICAL PROPERTIES

	58.0%	65.7%	74.0%	82.0%	88.3%	Production
Measured Thickness (μ inches)	158	158	138	118	118	118
Bulk Coating Density (g/cm^3)	1.860	2.280	2.110	2.542	2.453	2.649
Real Matrix Density (g/cm^3)	1.155	1.138	1.112	1.067	0.996	1.078
Apparent Porosity (%)	9.89	0.072	18.1	13.7	26.0	7.98
Particle Volume Fraction (%)	22.5	31.2	32.5	43.4	45.1	44.3
Pigment Volume Concentration (%)	25.0	31.2	39.7	50.3	61.0	48.1
Average Roughness (nm)	7.1	6.7	6.3	4.9	3.7	6.5
Apparent Gloss – 60° (%)	103	119	145	155	160	142

Appendix

Section I

These tools were originally derived for applications in advanced composite manufacturing research[8] but work equally well here. A magnetic coating, like most other coatings, is made up of a variety of component ingredients. If the resin and all other additives excluding the magnetic particles are treated as the binder (or matrix) then a coating basically consists of two portions by weight (particles and matrix) and three portions by volume (particles, matrix and porosity).

Symbol designation for coating components

W = weight of coating sample
w_p = weight of particles
w_m = weight of matrix
V = volume of coating sample
v_p = volume of particles
v_m = volume of matrix
v_a = volume of pores & voids

ρ_c = bulk coating density
ρ_m = real matrix density
ρ_p = particle density

Definition of component weight fractions

particle weight fraction

$$p_w = \frac{w_p}{W}$$

matrix weight fraction

$$m_w = \frac{w_m}{W}$$

Definition of component volume fractions

particle volume fraction

$$p_v = \frac{v_p}{V}$$

matrix volume fraction

$$m_v = \frac{v_m}{V}$$

porosity fraction

$$a = \frac{v_a}{V}$$

The sum of components by weight is equal to the coating weight

$$w_p + w_m = W$$

from which it follows

$$p_w + m_w = 1$$

The sum of components by volume is equal to the coating volume

$$v_p + v_m + v_a = V$$

from which it follows

$$p_v + m_v + a = 1$$

Volume fractions can be expressed in terms of their respective weight fractions. Since

$$\rho_p = \frac{w_p}{v_p} = \frac{p_w W}{p_v V} = \frac{p_w}{p_v}\rho_c$$

then

$$p_v = p_w \frac{\rho_c}{\rho_p}$$

Likewise,

$$m_v = m_w \frac{\rho_c}{\rho_m}$$

Bulk coating density can be written in terms of component weight fractions, component densities and the porosity:

$$\rho_c = \frac{W}{v_p + v_m + v_p} = \left[\frac{p_w}{\rho_p} + \frac{m_w}{\rho_m}\right]^{-1}(1-a)$$

which can be rearranged to give the porosity or void volume fraction,

$$a = 1 - \rho_c\left[\frac{p_w}{\rho_p} + \frac{m_w}{\rho_m}\right]$$

The matrix density can be found using a similar method as that shown above for bulk coating density. If the subscripts r, s, l, c, f, etc... represent resin, surfactants, lubricants, carbon, fungicide, etc... respectively then

$$\rho_m = \frac{w_m}{v_r + v_s + v_l + \ldots} = \frac{r_w\rho_r + s_w\rho_s + l_w\rho_l + \ldots}{w_m}$$

As described earlier, p_v is the volume fraction of particles within the total coating volume consisting of particles, matrix and porosity. However, the pigment (or particle) volume concentration PVC , is defined as the volume fraction of particles in the coating made up only of particles and matrix. Pores, whether present or not, are not considered in the definition of PVC, hence

$$PVC = \frac{p_v}{p_v + m_v} = \left[1 + \frac{m_w}{p_w}\cdot\frac{\rho_p}{\rho_m}\right]^{-1}$$

APPENDIX

Section II

Due to the variety of unit systems used in the field of magnetostatics, a brief description of units used in this report is recommended here. In the cgs-emu system of units, the magnetizing field H is measured in Oersteds (Oe) and the magnetic induction B is given in Gauss (G) where one Oersted is defined as being equal to one Gauss, 1 Oe = 1 G. Also, the fundamental unit of magnetic moment, the Bohr magneton μ_B, is defined in terms of electromagnetic units (emu),

$$1\mu_B = 9.274 \times 10^{-21}\text{erg/Gauss} = 9.274 \times 10^{-21}\text{emu}$$

It has been determined that each magnetic Cr^{+4} atom in the crystal structure of CrO_2 has a moment of 2.03 μ_B (18.826×10^{-21} emu) associated with it [4]. The magnetization M of a material is defined as magnetic moment per unit volume in units of emu/cm^3, which is converted into Gauss when multiplied by 4π. Vendor reported values of "saturation moment" σ_s as measured on bulk particles in units of emu/gram can be converted into Gauss when the magnetic particle density ρ_p is known. The saturation magnetization M_s associated with a single particle is then

$$\sigma_s\ (\text{emu/g}) \quad X \quad \rho_p\ (\text{g/cm}^3) \quad X \quad 4\pi \quad = \quad M_s\ (\text{G})$$

This value when multiplied by the packing fraction and squareness of a coating gives the bulk remanent magnetization associated with the coating. Gauss is the cgs-emu unit for magnetic flux ϕ per unit area of magnetic field and is defined as one Maxwell per square centimeter or 1 Mx/cm^2. Hence, all three fields B, H and M can be expressed in units of G (or Oe) and the familiar Maxwell relation can often be written simply as B = H + M or in general,

$$B = aH + bM$$

where a and b can be any unit conversion constants including one.

REFERENCES

[1] Dupont Chromium Dioxide Magnetic Crystals - Product Information, Information Storage Division, Wilmington, DE, (1988)

[2] "Magnetic Characterization Of Iron Oxide Dispersions", Randy Lee, Graham Magnetics Inc., (1992)

[3] "The Complete Handbook of Magnetic Recording", Finn Jorgensen 3rd Ed., (1988)

[4] "The Chemical And Physical Properties Of CrO_2 And Tetravalent Chromium Oxide Derivatives", B.L. Chamberland, University Of Connecticut, Department Of Chemistry, Storrs, Connecticut, (1977)

[5] "Paint Flow And Pigment Dispersion", Temple C. Patton, (1979)

[6] "Measurement Of Interaction Fields In Particle Tapes By Linearization Of The Henkel Plot", X. He, C. Alexander Jr. and M.R. Parker, Center For Materials For Information Technology, University Of Alabama, Tuscaloosa, AL, (1992)

"Phenomenology Of δM Curves And Magnetic Interactions", Xiaodong Che and H. Neal Bertram, Center For Magnetic Recording Research, University Of California, San Diego, (1992)

[7] "Introduction To Solid State Physics", C. Kittel, (1976)

[8] "Relationships In Carbon-Carbon Processing", Randy Lee, LTV Aerospace & Defense, Space Shuttle Program, (1987)